Research Article | Vol. 27, No. 16 | 5 Aug 2019 | OPTICS EXPRESS 22994
Optics EXPRESS

Regulation of lipid droplets in live preadipocytes using optical diffraction tomography and Raman spectroscopy

CHAO-MAO HSIEH,[1,7] PATRICIA YANG LIU,[1,2,7] LIP KET CHIN,[1,8] JING BO ZHANG,[3] KUAN WANG,[3,4] KUNG-BIN SUNG,[5] WEE SER,[1,9] TARIK BOUROUINA,[6] YAMIN LEPRINCE-WANG,[2] AND AI-QUN LIU[1,10]

[1]*School of Electrical & Electronic Engineering, Nanyang Technological University, 50 Nanyang Avenue, 639798, Singapore*
[2]*Université Paris-Est, UPEM, F-77545 Marne-la-Vallée, France*
[3]*Nanyang Environment & Water Research Institute, Nanyang Technological University, 1 Cleantech Loop, 637141, Singapore*
[4]*College of Biomedical Engineering and Taipei Cancer Center, Taipei Medical University, No. 250, Wuxing Street, Xinyi District, Taipei 11031, Taiwan*
[5]*Department of Electrical Engineering, National Taiwan University, No. 1, Section 4, Roosevelt Rd, Da'an District, Taipei 10617, Taiwan*
[6]*Université Paris-Est, ESYCOM, ESIEE, F-93162 Marne-la-Vallée, France*
[7]*Co-first authors with equal contribution*
[8]*lkchin@ntu.edu.sg*
[9]*ewser@ntu.edu.sg*
[10]*eaqliu@ntu.edu.sg*

Abstract: Lipid droplets have gained strong interest in recent years to comprehend how they function and coordinate with other parts of the cell. However, it remains challenging to study the regulation of lipid droplets in live preadipocytes using conventional microscopic techniques. In this paper, we study the effects of fatty acid stimulation and cell starvation on lipid droplets using optical diffraction tomography and Raman spectroscopy by measuring size, refractive index, volume, dry mass and degree of unsaturation. The increase of fatty acids causes an increase in the number and dry mass of lipid droplets. During starvation, the number of lipid droplets increases drastically, which are released to mitochondria to release energy. Studying lipid droplets under different chemical stimulations could help us understand the regulation of lipid droplets for metabolic disorders, such as obesity and diabetes.

1. Introduction

Lipid is an essential source of energy for human body, which is mainly stored in the form of lipid droplets (also known as lipid bodies or adiposomes) [1]. Lipid droplets are formed within the bilayer membrane of endoplasmic reticulum with external free fatty acids (non-esterified fatty acids) [2]. They are highly dynamic organelles that play a crucial role in energy storage [3–6] that also involved in many cellular functions, including lipid storage and metabolism. They also act as a source of membrane lipid for membrane maintenance and formation. Dysregulation of lipid droplets will cause metabolic disorders, leading to diseases such as obesity, fatty liver or diabetes [7]. Therefore, the regulation of lipid in adipocyte is one of the emerging research targets to tackle obesity and diabetes.

Lipid droplets consist of a hydrophobic core of neutral lipids, such as triacylglycerols, diacylglycerols or sterol esters, whereby fatty acids in lipid droplets exist in the form of triglyceride or diglyceride [8], and the rest have other functions such as the source of membrane lipid or hormone generation [9]. Fatty acids can be categorized into saturated,

#362798 https://doi.org/10.1364/OE.27.022994
Journal © 2019 Received 26 Mar 2019; revised 14 May 2019; accepted 24 May 2019; published 29 Jul 2019

Optics EXPRESS

monounsaturated and polyunsaturated fatty acids. Different fatty acids in a daily meal could affect the total body fat, i.e., the regulation of lipid droplets in cells, which is critical to maintain cellular functions and metabolic order. For example, docosahexaenoic acid (DHA), which is a polyunsaturated fatty acid, with a 22-carbon chain and 6 cis double bonds (C22:6) was found to inhibit the differentiation of various preadipocytes [10]. Therefore, it is critical to study the effect of fatty acid stimulation on the composition and concentration of lipid droplets in the cell.

Unfortunately, it is challenging to measure the differences in single lipid droplets from live cells in multi-parameter studies by microscopic approaches or biochemical analytical techniques. Fluorescence and phase contrast microscopies can identify lipid droplets but cannot provide quantitative information with sufficient details to study the changes of lipid droplet due to micro-environmental stimulations. Downstream biochemical analytical techniques such as Western blot require the collection of lipid droplets that make live cell monitoring impossible. As a result, a novel approach with multiple quantitative parameters is demanded to study the regulation of lipid droplets in live preadipocytes under different microenvironmental stimulations.

In this paper, we report the practical application of optical diffraction tomography and Raman spectroscopy to study the regulation of lipid droplets in live mouse embryonic 3T3-L1 preadipocytes under the stimulation of different fatty acids and the depletion of serum (starvation). Multiple parameters of the lipid droplets are studied using optical diffraction tomography (ODT), including size, refractive index (RI), volume and dry mass [11–14]. Since it is well known that fatty acids with long carbon chain and a high ratio of double bonds have a higher RI, we hypothesize that RI could be a potential parameter to analyze lipid droplets. Due to the distinctively higher RI of lipid droplets, three-dimensional (3D) RI imaging using ODT can provide quantitative information of lipid droplets in live cells without staining [15,16]. In addition, we can study the content of each lipid droplets with the measured dry mass. To further analyze the composition of fatty acids in single lipid droplets, Raman spectroscopy is used. The rich supply of C-H and C = C chemical bond in triglycerides and sterol esters, which are the primary components in lipid droplets, leads to the strong Raman signals at specific vibrational signature of molecules. The degree of unsaturation of fatty acids in lipid droplets can be determined by the ratio ($I_{1,660}/I_{1,450}$) of the intensity of the 1,660 cm^{-1} band (C = C) to the 1,450 cm^{-1} band ($-CH_2$) [17–20]. The study of lipid droplets in single live cells under different fatty acid stimulations will pave a new understanding in the regulation of lipid droplets for metabolic disorders such as obesity and diabetes, which are the primary lifestyle diseases, especially in developed countries.

2. Experimental section

2.1. Optical diffraction tomography

The optical setup is presented in Fig. 1, which is based on Mach-Zehnder interferometry whereby a laser beam (λ = 488 nm, 100 mW, Sapphire SF 488, USA) is split by a beam splitter. One arm of the light beam passes through the sample, and the other arm of it passes through the reference path. Both beams combine through another beam splitter to form a two-beam interferogram. The hologram is captured by CMOS camera (100 Hz at 1,024 × 1,024 pixels, pco.edge 5.5, PCO Inc, German). The complex optical fields of the sample, containing both amplitude and phase information, are recorded at various illumination angles. A high NA objective lens (oil immersion, 60 × , NA 1.4, Nikon) and a high NA condenser (NA 1.4, UPLSAPO, Olympus) are used to maximize the range of illumination angles. Moreover, the maximum illumination angle generated by two galvanometer scanners (dynAXIS; SCANLAB Inc., German) is limited to around 65° in PBS solution at 488 nm.

Optics EXPRESS

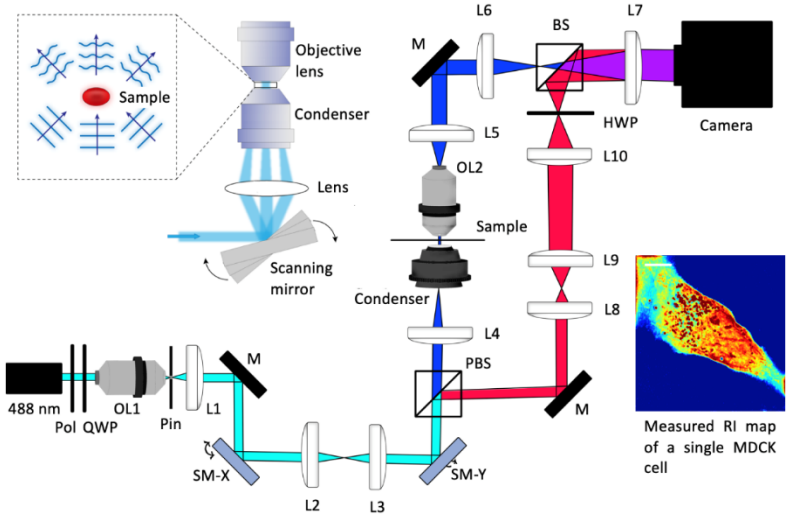

Fig. 1. Schematic illustration of optical diffraction microscope for 3D RI measurement. Pol: polarizer; QWP: quarter wave plate; HWP: Half-wave plate; OL1, OL2: objective lens; Pin: pinhole; BS: Beam splitter; PBS: polarizer beam splitter; M: mirror; L1-L9: lens; SM-X, SM-Y: Scanning mirror. Inset on the right shows the measured RI map of a single (Madin-Darby Canine Kidney) MDCK cell.

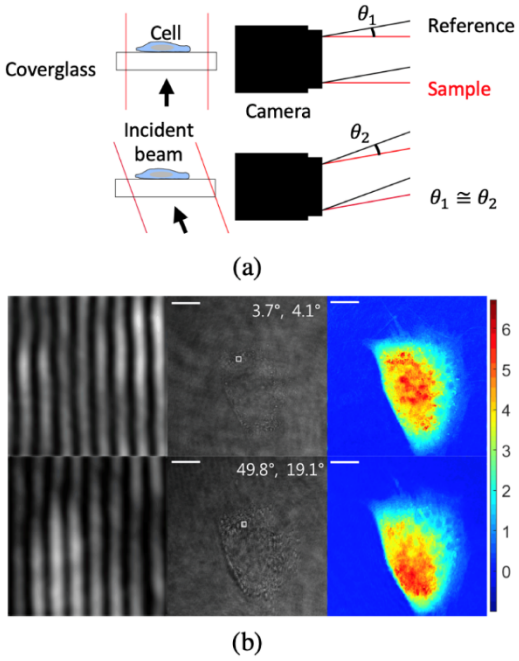

Fig. 2. Digital holograms contained interference fringe with fixed spatial frequency at various illuminated angles. (a) Angle between two light beams entering into camera remained similar when illuminated angle is changed. The spatial frequency of interference fringe remains the same. (b) hologram and phase image of a single cell. Scale bar: 10 μm. Color bar: phase delay at 488 nm.

A combination of optical diffraction tomography and projection on convex sets with total variation minimization algorithm (ODT-POCS&TV) has been implemented for the system [21]. The reconstruction principle and process can be referred from the published paper [22].

Optics EXPRESS

Briefly, a complex optical field of the sample illuminated at a particular angle is mapped on the surface of Ewald sphere in 3D Fourier space from phase imaging based on Fourier diffraction theorem. Inverse Fourier transform of the 3D Fourier space containing all information from the sample scatter field at various illumination angles is calculated to obtain the 3D RI distribution. The missing area of the sample out of illumination angles due to the limited numerical aperture of the objective lens is filled by the iterative non-negativity algorithm. The RI and size of the samples are retrieved from the 3D RI distribution. To decrease the number of captured frames and minimize the vibration effect on phase-shifting algorithm, the system is redesigned by scanning the sample beam and reference beam simultaneously to generate a high-frequency interferogram with the fixed fringe pattern at any scanning angle as shown in Fig. 2 to fit the algorithm of Hilbert transform microscope [23]. The sample is illuminated at 500 different angles in 2D to generate 500 frames recorded by a camera in 10 seconds.

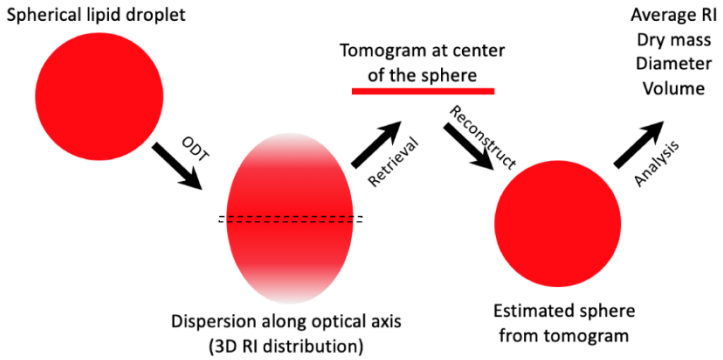

Fig. 3. Illustration of the estimation process of analyzing lipid droplets in cells from RI tomogram. Due to the worse resolution along optical axis away from focal plane, the center of the lipid droplet is more accurate than the other planes. Hence, the lipid droplet is reconstructed from its central plane to avoid the imaging artefact.

Since the refractive index of lipid droplets is significantly different from that of cytoplasm, we choose the threshold of $n > 1.341$ (PBS) and $n > 1.380$ to distinguish cytoplasm and lipid droplets, respectively. Then, segmentation method is implemented using MATLAB software to isolate and calculate the number of lipid droplets, following with analysis on each lipid droplet. Volume and dry mass of lipid droplets can be retrieved from the 3D RI distribution of 3T3-L1 cells [16]. The area of lipid droplets is determined by integrating all the voxels in the selected region with the RI greater than 1.380. However, the resolution of the system decreases along the optical axis, and spherical lipid droplets will become oval in shape. The artefact of RI and volume out of the central focal plane could induce errors in the value estimation. Hence, we retrieve the central plane of lipid droplets and make an estimated sphere based on the information from the selected area as illustrated in Fig. 3. In order to use such estimation, lipid droplets are assumed to be spherical and their central plane is approximately the same as the focal plane of the microscope objective. Since cells are well attached on the surface of the glass coverslip, the spatial distribution of lipid droplets in cells is limited in a small range at the focal plane.

The RI value of lipid droplet is linearly proportional to the lipid concentration in it, i.e., $n(x, y, z) = n_m + \alpha C(x, y, z)$, where n_m is the RI of external medium, C represents the concentration and α is a constant. Hence, the dry mass of each lipid droplet can be determined from concentration, i.e. $m = \iiint (n(x, y, z) - n_m)/\alpha$ where $\alpha = 0.135$ mL/g for lipid [12,21].

Optics EXPRESS

2.2. Raman spectroscopy and confocal microscopy

Raman spectra of lipid droplets in cells are measured using a 100 × oil immersion objective (Nikon) in a Raman microscope (μRaman-532TEC, Technospex) with 532 nm laser light source. Each lipid droplet takes around 4 to 8 seconds to obtain a stable and strong Raman signal. For confocal imaging, the 3T3-L1 cells are stained with BODIPY 493/503 and Rhodamine 6G (R6G) for 10 min in a serum-free medium and followed by three washes with PBS. 488-nm and 563-nm laser lines are used to excite BODIPY and Rhodamine 6G (R6G), respectively. Cells are examined using a 100 × oil immersion objective (Leica) in a scanning confocal microscope (TCS SP8, Leica) with a pinhole of 0.31 AU.

2.3. Characterization of ODT and Raman spectroscopy

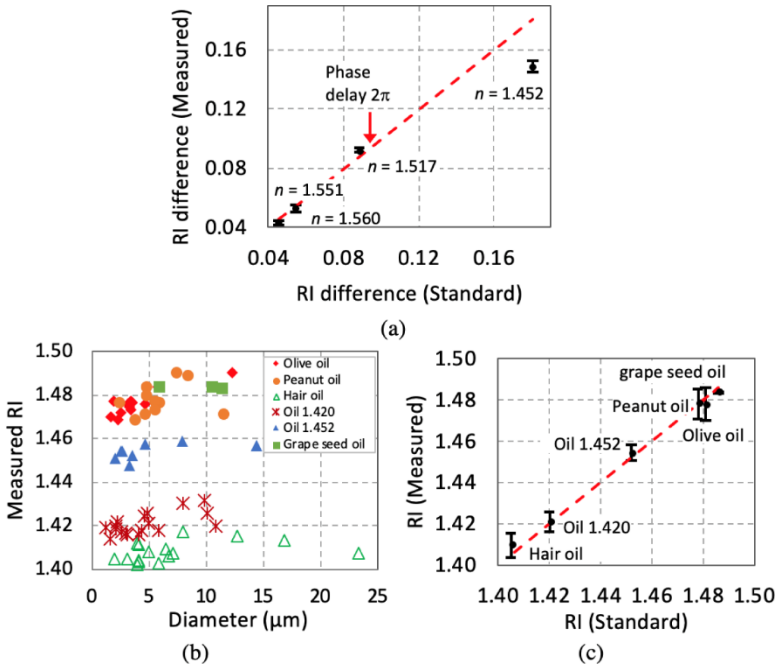

Fig. 4. Characterization of ODT system with (a) 5-μm polystyrene bead in immersion oil (sample size of 20 beads), (b) measured diameter and RI of different oil droplets in PBS using ODT and (c) comparison between measured and standard RI of different oil droplets.

The ODT system is firstly calibrated for its imaging magnification and resolution. The edge definition and RI precision are measured by using standard 5-μm polystyrene beads (Polysciences, n = 1.6054 at λ = 488 nm) suspending in RI liquids (Cargille, n = 1.425, 1.517, 1.551 and 1.560 at λ = 486 nm) as shown in Fig. 4(a). Edge response approach is used to calculate the spatial resolution, i.e. the distance at the edge of the bead whereby RI changes from 10% to 90% of total RI difference ($n_{bead} - n_{liquid}$). The measured RI has a standard deviation ± 0.15%, and the spatial resolution calculated from edge response is estimated to be approximately 210 nm and 350 nm in lateral (x-y) and axial (z) directions. Subsequently, since the RI difference between lipid droplets and cytoplasm is much larger compared to the one between the polystyrene bead and RI liquids, the RI of pure oil droplets (hair oil, n = 1.405; RI liquids, n = 1.420 and 1.452; peanut oil, n = 1.478; olive oil, n = 1.481; grapeseed oil, n = 1.486) suspended in PBS solution (n = 1.341) are measured to mimic lipid droplets in live cells as shown in Fig. 4(b). The pure oil droplets with different sizes are generated by ultrasonication, whereby pure oil is first mixed in PBS solution and then sonicated for 3 minutes in ultrasonic bath (D200H, MRC). The RI of the oils and PBS solution are measured using a standard Abbe refractometer (Abbemat 200, Anton Paar) as references. The measured

Optics EXPRESS

RI of various oil droplets match well with the standard RI measured by the Abbe refractometer as shown in Fig. 4(c). It is noted that oil droplets with higher RI difference as compared to the RI of PBS (e.g. peanut oil and olive oil) and large droplet size tend to be less accurate with larger variation (± 0.5%). This might be due to the phase error caused by large phase jump of more than 2π in the wrapped phase map [13]. However, since the size of most lipid droplets measured in the experiments is less than 3 μm in diameter as illustrated in Fig. 5, the ODT is sufficient for the study of lipid droplets in live preadipocytes under various biochemical stimulations.

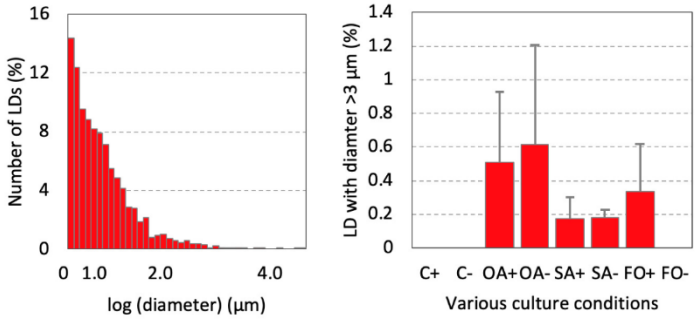

Fig. 5. (a) Size distribution of lipid droplets of cells fed with fish oil. (b) Percentage of lipid droplets with diameter larger than 3 μm under various culture conditions (sample size: 20 cells). C: control; OA: oleic acid; SA: stearic acid; FO: fish oil; + : with serum; -: without serum (cell starvation).

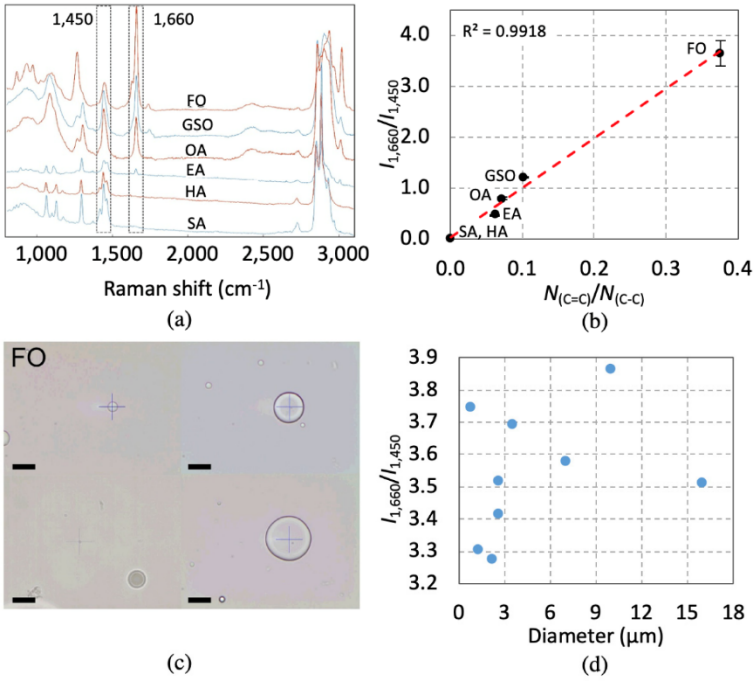

Fig. 6. Calibration of Raman spectroscopy. (a) Raman spectra of different fatty acids. (b) Intensity ratio $I_{1,660}/I_{1,450}$ with respect to the degree of unsaturation of fatty acid. FO: fish oil; GSO: grape seed oil; OA: oleic acid; EA: erucic acid; HA: hexanoic acid; SA: stearic acid. (c) Bright-field images of fish oil droplets with different sizes in PBS. Scale bar: 10 μm. (d) Analysis of the level of unsaturation of fish oil droplets.

Optics EXPRESS

To correlate measured RI of lipid droplets and its composition, Raman spectrum of lipid droplets is measured and the intensity ratio $I_{1,660}/I_{1,450}$ is determined. The Raman spectroscopy is first calibrated by measuring oil droplets with pure known fatty acids (docosahexaenoic acid C22:6, eicosapentaenoic acid C20:5, palmitoleic acid C16:1, linoleic acid C18:2, oleic acid C18:1, erucic acid C22:1, hexanoic acid C6:0 and stearic acid C18:0) in PBS solution. Based on the Raman spectra in Fig. 6, unsaturated fatty acid has higher intensity at 1,660 cm^{-1} band, and the results show that the ratio of C = C double bond to -CH_2 bond in the compound is linearly correlated to the intensity ratio $I_{1,660}/I_{1,450}$. Although smaller oil droplets generate weaker intensity, the intensity ratio is not distinctly affected.

2.4. Culture of 3T3-L1 preadipocytes and fatty acid stimulation

Mouse embryonic 3T3-L1 preadipocytes (CL-173, ATCC) are cultured in the growth medium (GM) that consists of high-glucose Dulbecco's modified Eagle medium (GIBCO) with 10% fetal bovine serum (Invitrogen). Subculture is implemented in 2 to 3 days when confluency reaches ~80%. To investigate cell viability, cells are cultured in petri-dish and stained with SYBR-Green (Invitrogen) and propidium iodide (PI; P3566; ThermoFisher Scientific). Stained 3T3-L1 cells are imaged with an inverted fluorescence microscope (Eclipse Ti-U; Nikon), and the number of cells is calculated from the image to determine the viability by comparing the number of cells at different time points.

Free fatty acids used in the experiments include fish oil (891611, GNC) that contains 60% docosahexaenoic acid (DHA) and 40% eicosapentaenoic acid (EPA), stearic acid (S4751; SIGMA), oleic acid (75096; SIGMA), hexanoic acid (153745; SIGMA), erucic acid (45629; SIGMA), olive oil, peanut oil, hair oil and grape seed oil from a local food company. Oleic acid, stearic acid and fish oil are added to the growth medium to stimulate the generation of lipid droplets in cells. Before adding these fatty acids into the growth medium, the free fatty acids (FFAs) are mixed with bovine serum albumin (BSA; A2153; SIGMA) to form BSA-FFA complexes. Briefly, FFA is added into 0.01 M NaOH solution for saponification at 70°C for 30 minutes. Then, the fatty acid salt is retrieved and added to PBS solution with 5% BSA. Finally, the BSA-FFA complex is added to GM (DMEM, 10% Fetal bovine serum, 1% penicillin and streptomycin) and starvation medium (SM; DMEM, 1% penicillin and streptomycin), and then filtered through a 0.2-μm syringe filter, forming the stock solution. 3T3-L1 cells are first cultured in GM on the coverslips overnight for attachment before various treatments. When most of the cells are fully attached to the surface of coverslips, the medium is rinsed and changed to fresh GM/SM. After treatment with different fatty acids in these media for 24 hours, cells are washed and dipped into PBS for observation.

3. Results and discussion

3.1. Effect of fatty acid stimulation on lipid droplets

Lipid droplets in a live cell can be identified by staining with BODIPY 493/503. Since the ODT is integrated with fluorescence imaging functionality, the RI and fluorescence emission of BODIPY dye in a single live cell can be obtained simultaneously as shown in Fig. 7(a). The results show that intracellular organelles with high RI are also emitting fluorescence signal. As a result, lipid droplets have higher RI than other intracellular organelles in preadipocyte cells, which make it easier to identify lipid droplets in the RI tomogram and simplify the study of lipid droplets based on RI under different biochemical stimulations. In addition, it is noted that the fluorescence intensity is moderately weak in correlation with RI value (R^2 = 0.243), indicating that it is relatively hard to study lipid droplets quantitatively purely based on fluorescence imaging.

Optics EXPRESS

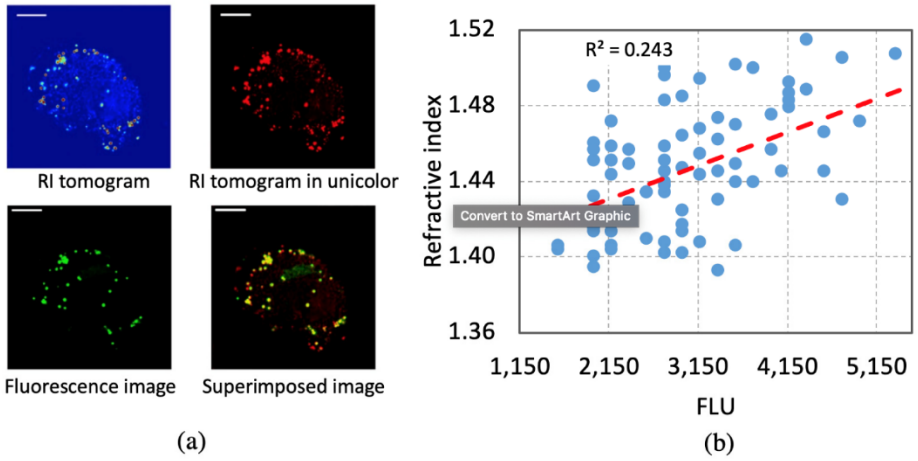

Fig. 7. RI measurement of lipid droplets. (a) RI tomogram and fluorescence image of lipid droplets stained with BODIPY. Scale bar: 10 μm. (b) RI with respect to fluorescence intensity of lipid droplets. A bin of 200 FLU value is used.

To investigate the effect on lipid droplet regulation in 3T3-L1 cells under fatty acid stimulation, four different culture conditions are performed, i.e. (1) without any fatty acids (control), (2) with 0.75 mM of monounsaturated oleic acid, (3) with 0.75 mM of saturated stearic acid, and (4) with 0.75 mM of polyunsaturated fish oil that consists of DHA and eicosapentaenoic acid (EPA). A sample size of 20 cells are investigated for each condition. The RI tomogram of 3T3-L1 cells under these four culture conditions are shown in Fig. 8(a), and the statistical data of the number, size, RI, degree of unsaturation ($I_{1,660}/I_{1,450}$) and dry mass are illustrated in Figs. 8(b)–8(e), respectively.

First, the regulation of lipid droplet generation in 3T3-L1 cells with oleic acid stimulation is studied. Oleic acid is commonly used in lipid droplet studies since it is one of the most abundant fatty acids found in cells [24]. Additional oleic acid will facilitate cells to form more and larger lipid droplets because cells will store the uptake free fatty acids in lipid droplets as the form of triacylglycerol to avoid the lipotoxicity [25,26]. Based on the experimental results in Fig. 8(b), the number and average size of lipid droplets increase with the addition of oleic acid from 24 ± 15 to 41 ± 15 and 0.8 ± 0.3 μm to 1.2 ± 0.5 μm, respectively. In term of RI as shown in Fig. 8(c), the difference in average RI of lipid droplets with the stimulation of oleic acid (n = 1.449 ± 0.020) is lower to the one without fatty acid (n = 1.450 ± 0.022). Similar results are observed based on Raman spectroscopy in Fig. 8(d), in which the difference in intensity ratio $I_{1,660}/I_{1,450}$ for lipid droplets with the stimulation of oleic acid (0.80 ± 0.04) is lower to the one without (0.88 ± 0.08) fatty acid. It is known that wild cells without the stimulation of fatty acids would covert glucose into fatty acids and store them in lipid droplets that consist of palmitic acid (C16:0), oleic acid (C18:1) and linoleic acid (C18:2) [24]. Their average refractive index is slightly higher than pure oleic acid. As the oleic acid increase in lipid droplets under stimulation, there is a decrease in RI, which matches with those presented using other techniques [27]. Although the RI of lipid droplets decreases, the average dry mass of lipid droplet under oleic acid stimulation increases as illustrated in Fig. 8(e), showing that the lipid droplets have higher intake of oleic acid.

Optics EXPRESS

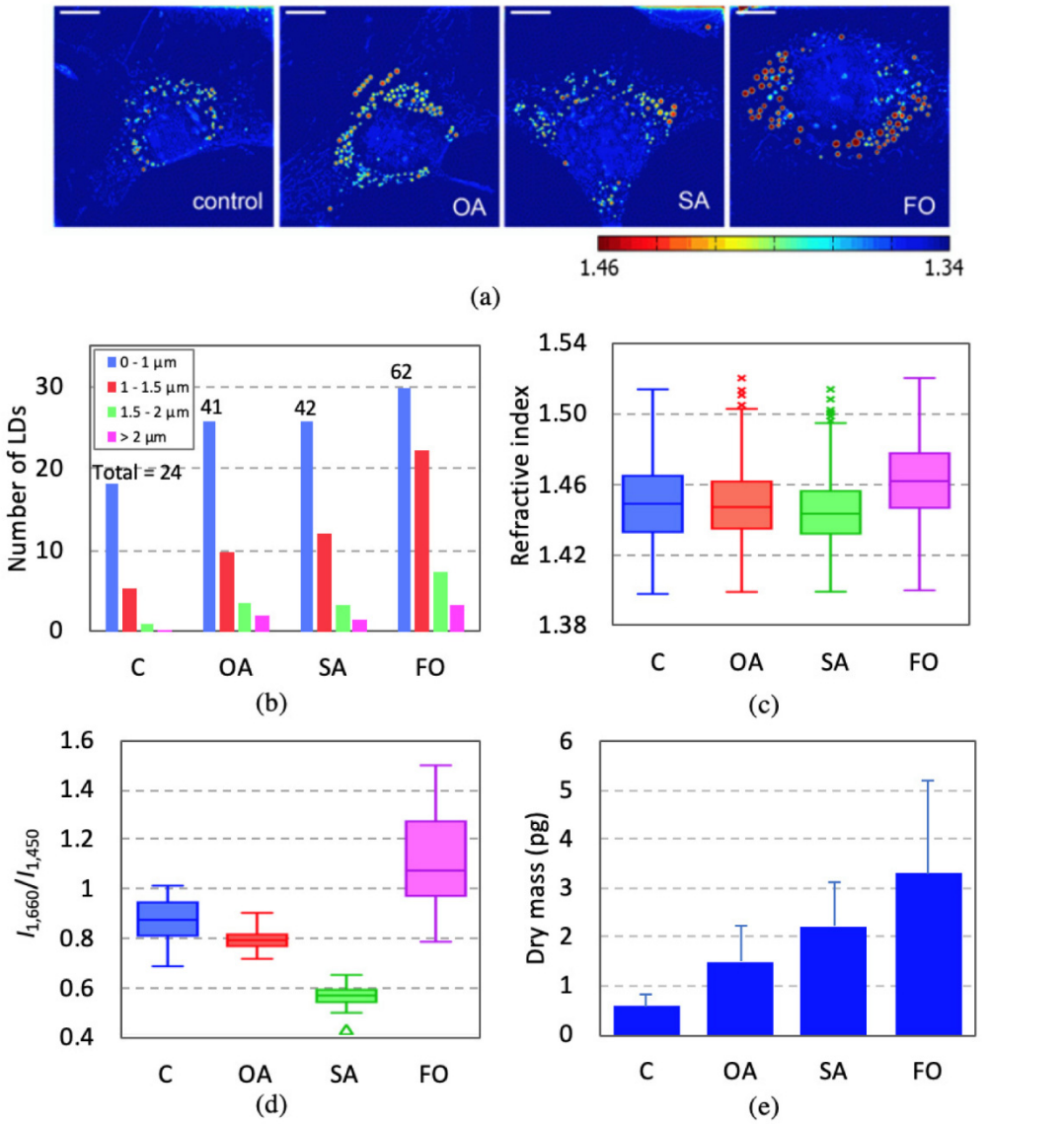

Fig. 8. Analysis of lipid droplets in cells with free fatty acid stimulation in full growth medium. (a) RI tomogram of 3T3-L1 cells under different fatty acid simulation conditions. Scale bar: 10 μm. Color bar: RI at 488 nm. OA: Oleic acid; SA: Stearic acid; FO: Fish oil. (b) Number, (c) RI distribution, (d) degree of unsaturation and (e) dry mass of lipid droplets under different fatty acid simulation conditions.

Next, the regulation of lipid droplet generation in 3T3-L1 cells with stearic acid and fish oil stimulation is studied. In general, the size and number of lipid droplets have statistically significant increase with the addition of fatty acids as illustrated in Fig. 8(b). In term of RI as shown in Fig. 8(c), lipid droplets in cells stimulated with stearic acid have the lowest mean value (n = 1.445 ± 0.019) while those with fish oil has the highest mean value (n = 1.461 ± 0.023). However, it is noted that the average RI of lipid droplets in cells stimulated with stearic acid is lower than those with oleic acid (n = 1.449 ± 0.020) but much higher than the RI of pure stearic acid (n = 1.429). On the contrary, the average RI of lipid droplets in cells stimulated with fish oil is higher than those with oleic acid but lower than the RI of pure fish

oil (n = 1.491). A similar trend is observed in Raman spectroscopy as shown in Fig. 8(d), whereby the intensity ratio $I_{1,660}/I_{1,450}$ for lipid droplets with the stimulation of stearic acid, oleic acid, and fish oil are 0.57 ± 0.04, 0.80 ± 0.04, and 1.14 ± 0.16, respectively. Both RI and Raman spectroscopy show that cells store additional fatty acids in lipid droplets, changing the composition of lipid droplets. Lipid droplets with higher content of unsaturated fatty acid have higher RI. However, the difference of RI and Raman signal between fish oil-fed cells and pure fish oil indicate that DHA and EPA are not the dominant type of fatty acid in lipid droplets. It could be that DHA and EPA are converted to a different form of lipid droplets in the fish oil-fed cells. The effect of saturated fatty acid on the formation of lipid droplets is less significant due to the possibility that saturated fatty acid is converted to unsaturated fatty acid before forming the lipid droplets [1]. Similarly, the dry mass of lipid droplets increases significantly in stearic acid and fish oil stimulation (Fig. 8(e)). These results reveal that the treatment of fatty acids increases the number and dry mass of lipid droplets. However, the change in composition depends on the type of fatty acid to be added to the cells, which is proven by the difference in RI and degree of unsaturation.

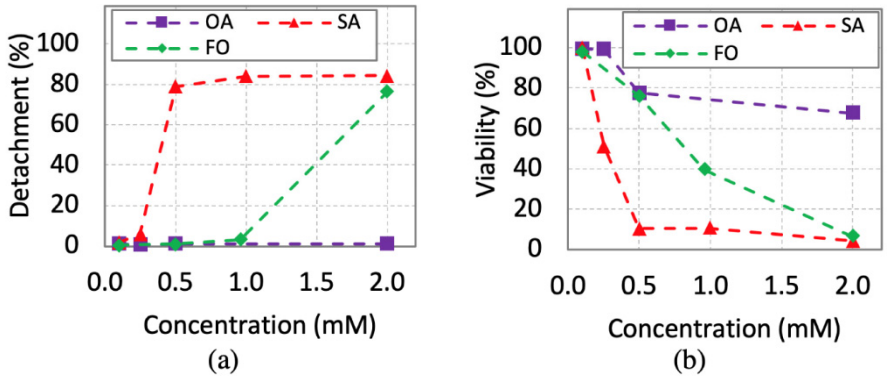

Fig. 9. (a) Detachment and (b) viability of 3T3-cells when treated with different fatty acids. OA: Oleic acid; SA: Stearic acid; FO: Fish oil.

It is noted that excess fatty acid is harmful to cells, especially saturated and polyunsaturated fatty acids that will cause lipotoxicity and induce cell apoptosis as illustrated in Fig. 9 [10,28]. The viability of cells is determined by using propidium iodide (red fluorescence dye) and SYBR-Green (green fluorescence dye) to label dead cells and live cells, respectively. From the results, it is observed that cell viability reduces with the stimulation of stearic acid and fish oil, which is more significant in a higher concentration of fatty acids. On the other hand, oleic acid has relatively less effect on cell viability.

3.2. Effect of cell starvation

Starved cells release lipid droplets to mitochondria for energy generation, which causes the decrease in size and number of lipid droplets in cells, but serum deprivation also induces autophagy-driven growth of lipid droplets [29]. For survival, cells will regulate lipid droplets during nutrient stress conditions. To monitor the regulation of lipid droplets in the cell during starvation, 3T3-L1 cells are sub-cultured with different free fatty acids. First, the effect of free fatty acid (a mixture of stearic acid, oleic acid, and fish oil at a ratio of 1: 1: 1) stimulation on the regulation of lipid droplets in 3T3-L1 cells are investigated by monitoring the size, RI, dry mass and number of lipid droplets after culturing the cells with the free fatty acids for 24 hours (0 hr of starvation is defined as the initial time point). After the treatment, cells are washed with PBS and cultured in serum-free medium without fatty acid to observe the effect of starvation on lipid droplet, and the parameters of lipid droplets are measured at different time points during starvation. Figure 10(a) illustrates the size and RI distribution of lipid

Optics EXPRESS

droplets at different time points. With the 24-hour stimulation of free fatty acid, the number of lipid droplets increases significantly from 31 ± 18 to 182 ± 67 compared to those without treatment of free fatty acid as shown in Fig. 10(b). The number and average dry mass of lipid droplets are decreasing and depleted after 78 hours of cells cultured without the stimulation of free fatty acid as illustrated in Figs. 10(b) and 10(c). Similar trends are observed in the case with fatty acid stimulation, i.e. decreasing number and dry mass of lipid droplets with respect to time. It is possible that, during starvation, lipid droplets are released to mitochondria for free fatty acid uptake to generate energy [22]. Remaining lipid droplets after 78 hours starvation are smaller in size and lower in RI as shown in Fig. 10(a).

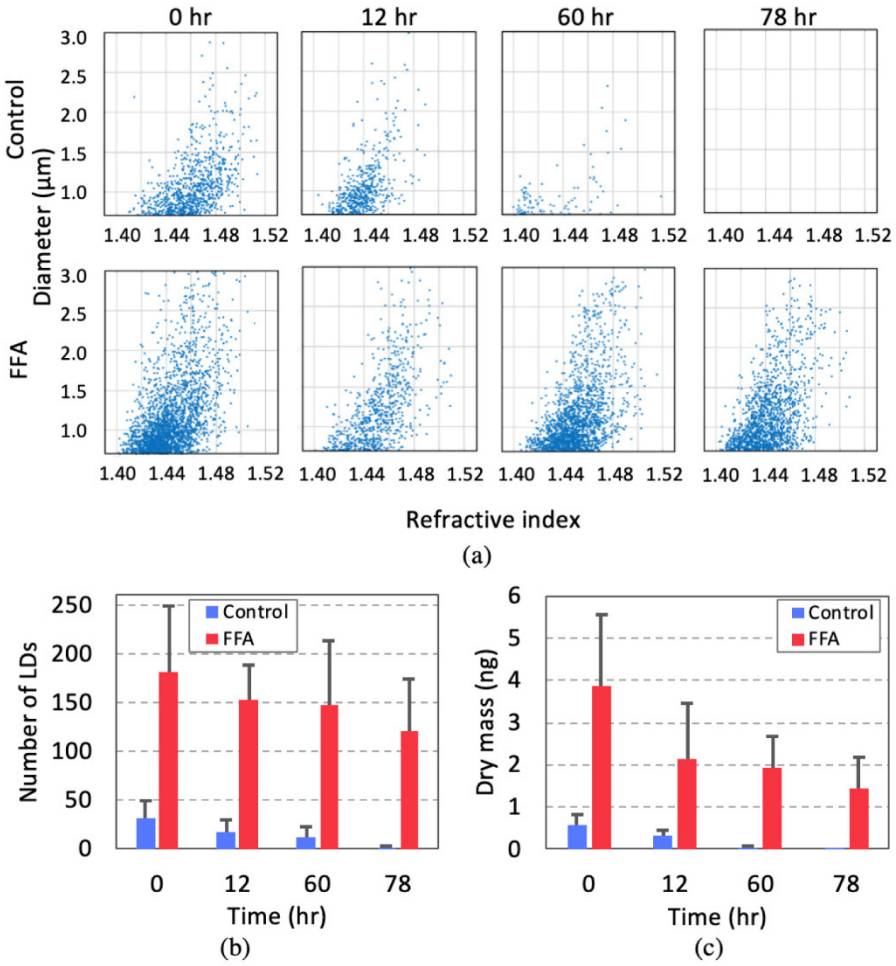

Fig. 10. Time-lapse analysis of lipid droplets in cells during starvation after free fatty acid stimulation in full growth medium. Statistical analysis of (a) size of lipid droplets and RI distribution, (b) number and (c) dry mass of lipid droplets. FFA: mixture of stearic acid, oleic acid, and fish oil.

Next, the controlled uptake of different kinds of fatty acids and the regulation of lipid droplets by the cells are investigated by culturing 3T3-L1 cells in serum-free medium supplemented with the BSA-fatty acid complex. Figure 11(a) shows the RI tomograms of 3T3-L1 cells under different conditions: normal culture medium (C+), serum-free medium (C-), serum-free medium with the addition of oleic acid (OA-), stearic acid (SA-) and fish oil (FO-), respectively. Figure 11(b) presents the average number of lipid droplets in starved cells under different fatty acid stimulations. It shows that oleic acid induces the generation of lipid

Optics EXPRESS

droplets significantly (68 ± 35) but not in the case of stearic acid (32 ± 20) and fish oil (24 ± 21). Based on Fig. 11(c), the average RI of lipid droplets in starved cells cultured with the three different fatty acids (n = 1.429 ± 0.018 in oleic acid, 1.432 ± 0.019 in stearic acid, 1.438 ± 0.020 in fish oil) is lower than those in cells cultured in growth medium (n = 1.448 ± 0.020 in oleic acid, 1.445 ± 0.019 in stearic acid, 1.461 ± 0.023 in fish oil). By comparing the intensity ratio $I_{1,660}/I_{1,450}$ in Fig. 11(d), the degree of unsaturation in lipid droplets for starved cells cultured with oleic acid (0.72 ± 0.04) and stearic acid (0.31 ± 0.08) decreases but it increases for the case of fish oil (1.58 ± 0.29). Under fish oil stimulation, the degree of unsaturation increases but RI decreases, which indicates that the lipid droplets become less dense with polyunsaturated fatty acids as the primary component.

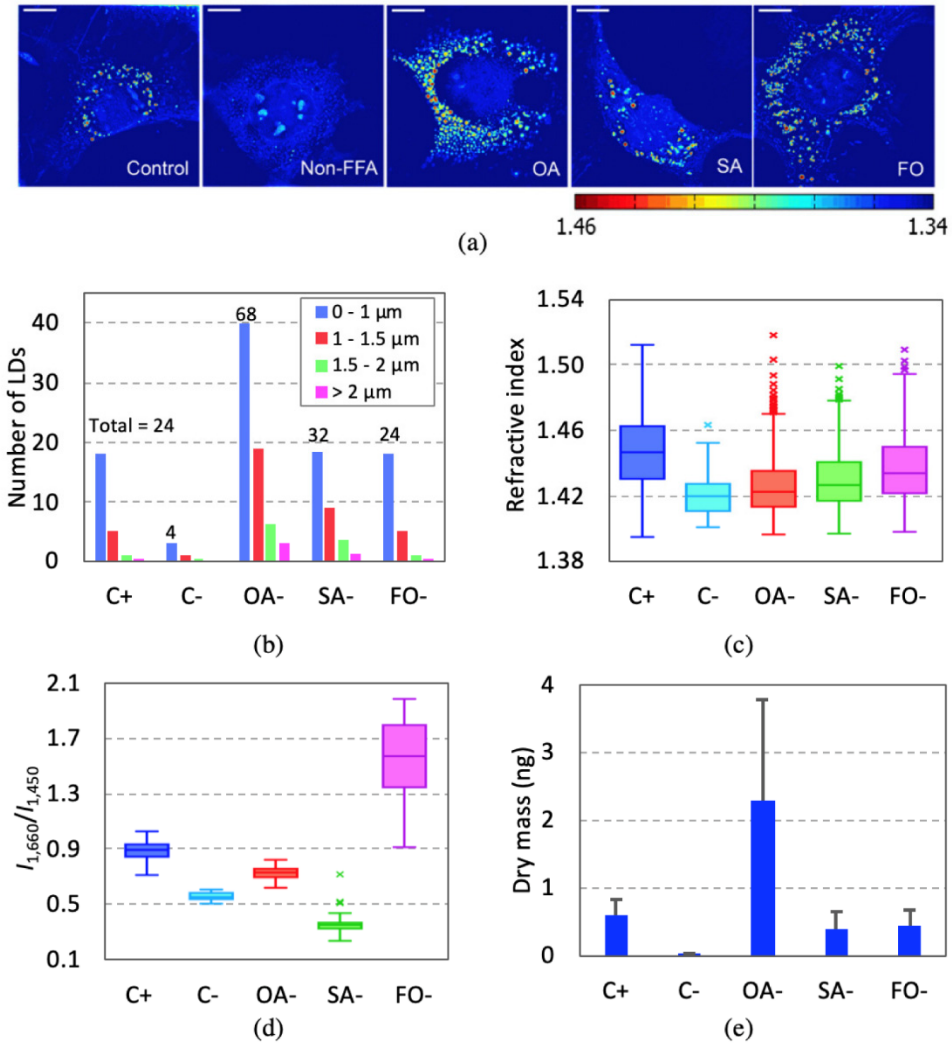

Fig. 11. Analysis of lipid droplets in cells with the treatment of different fatty acid under starvation. (a) RI tomogram of 3T3-L1 cells under different stimulation conditions. Scale bar: 10 μm. Color bar: RI at 488 nm. Non-FFA: no treatment with fatty acid; OA: Oleic acid; SA: Stearic acid; FO: Fish oil. (b) Number, (c) RI distribution, (d) degree of unsaturation and (e) dry mass of lipid droplets. C+ : normal culture medium; C-: serum-free medium; OA-: oleic acid in serum-free medium; SA-: stearic acid in serum-free medium; FO-: fish oil in serum-free medium.

Optics EXPRESS

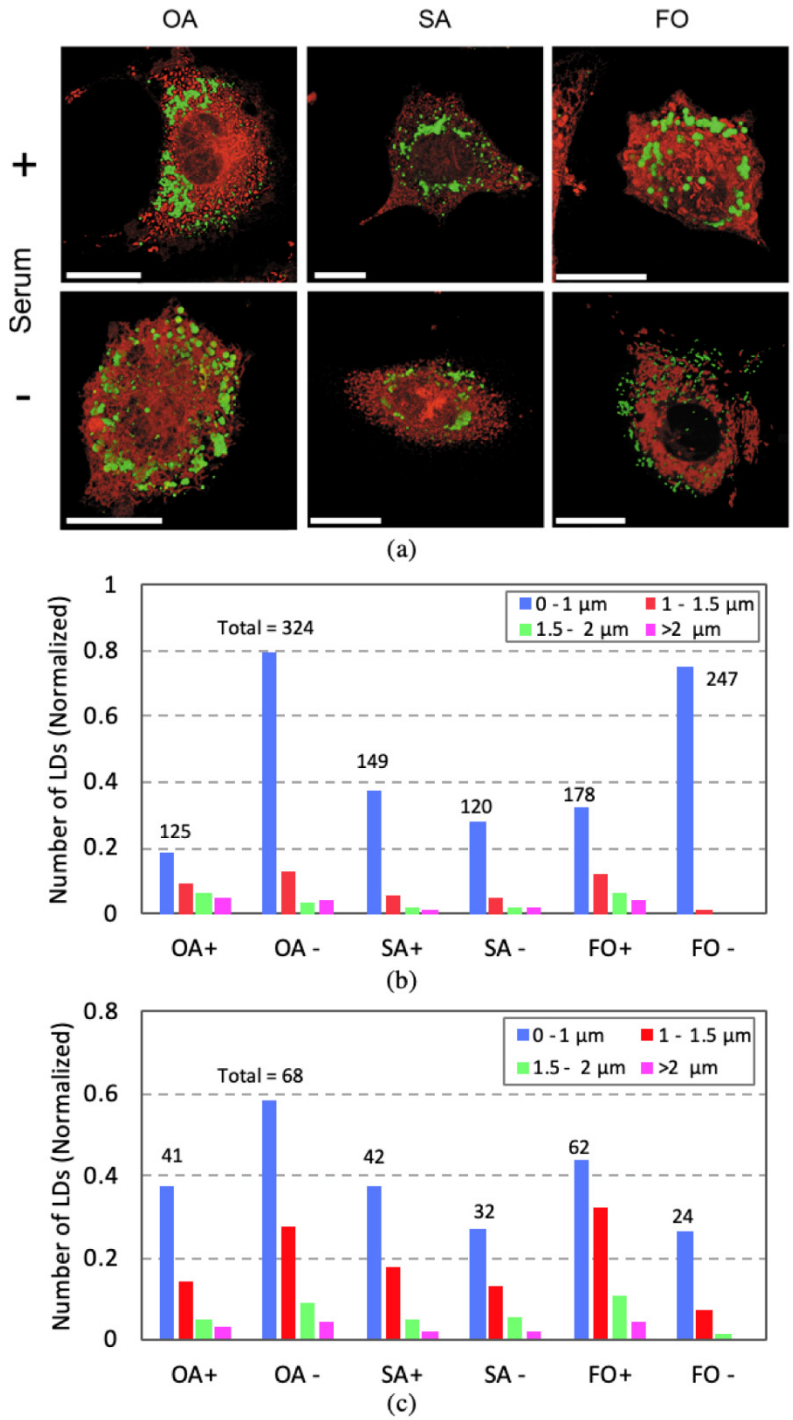

Fig. 12. Confocal imaging of 3T3-L1 cells and size distribution. (a) Confocal image of the 3T3-L1 cell (Green: BODIPY 493/503; Red: Rhodamine 6G, R6G) without/with serum in growth culture medium under different stimulation conditions. OA: Oleic acid; SA: Stearic acid; FO: Fish oil. Scale bar: 20 µm. Statistical analysis of number and size of lipid droplets using (b) confocal microscope and (c) ODT microscope. The number of lipid droplets is normalized with the maximum total number, i.e. 324 and 68 for (b) and (c), respectively.

Optics EXPRESS

By analyzing the total dry mass of lipid droplets in Fig. 11(e), starved cells treated with oleic acid not only generate more lipid droplets (all size range) but also lead to a higher total dry mass in the lipid droplets. The dry mass of lipid droplets decreases in starved cells fed with stearic acid while the number of droplets increased. However, fish oil does not significantly stimulate the generation of tiny lipid droplets nor does it increase the total dry mass. Due to the lower RI and a higher degree of unsaturation, this result suggests that the lipid droplets in starved cells become less dense under fish oil stimulation. However, it remains unknown why the lipid droplets become less dense with a high degree of unsaturation. One possible reason might be long chain unsaturated or monounsaturated fatty acids are consumed first as energy fuel of mitochondria while polyunsaturated fatty acids remain. These results indicate that monounsaturated fatty acids are crucial sources of lipid droplet formation in starved cells comparing to saturated and polyunsaturated fatty acids, and polyunsaturated fatty acids are not the major source of energy use in starved cells.

To evaluate the number of lipid droplets more precisely, line-scanning confocal microscope is used to image lipid droplets and cytoplasm in cells by staining with BODIPY and R6G, respectively. Figure 12(a) illustrates the confocal images of 3T3-L1 cells under different stimulation conditions. The average number and size of lipid droplets measured by confocal microscope and ODT are presented in Figs. 12(b) and 12(c). The number of lipid droplets increases with oleic acid addition but decreases with stearic acid. For fish oil stimulation, the number of tiny lipid droplets (<1 μm) increases but large lipid droplets (> = 1 μm) decreases. It indicates that, unlike oleic acid stimulation, cells can generate tiny lipid droplet but cannot produce larger droplets under fish oil stimulation. The difference in number observed between ODT and confocal microscope could be due to the diffraction-limit resolution. Tiny lipid droplets beneath the resolution limit are difficult to be observed by ODT. However, the decreases in the number of larger lipid droplets in stearic acid and fish oil, and increases in oleic acid are corresponding to the result of ODT.

4. Conclusion

In conclusion, we demonstrate the application of optical diffraction tomography to investigate the number, size, RI and dry mass of lipid droplets, and Raman spectroscopy to study the composition of fatty acid in the lipid droplets. The regulation of lipid droplets in mouse embryonic 3T3-L1 preadipocytes under the stimulation of different fatty acids and the depletion of serum (starvation) is studied. The size and number of lipid droplets in cells increase under fatty acid stimulation. Larger lipid droplets are found in cells fed with monounsaturated fatty acid (oleic acid) than those with saturated (stearic acid) and polyunsaturated fatty acid (fish oil). Both RI and Raman spectroscopy show that lipid droplets with higher content of unsaturated fatty acid have higher RI. For cell under starvation, the number of lipid droplets increases significantly under fatty acid stimulation. For the case with fish oil, RI decreases and degree of unsaturation increases, suggesting that the lipid droplets become less dense. The study of lipid droplets in single live cells under different fatty acid stimulations will pave a new path to understand the regulation of lipid droplets for metabolic disorders such as obesity and diabetes.

Funding

Singapore National Research Foundation under the Competitive Research Program (NRF-CRP13-2014-01).

References

1. P. T. Bozza and J. P. Viola, “Lipid droplets in inflammation and cancer,” Prostaglandins Leukot. Essent. Fatty Acids **82**(4-6), 243–250 (2010).
2. K. M. Nieman, I. L. Romero, B. Van Houten, and E. Lengyel, “Adipose tissue and adipocytes support tumorigenesis and metastasis,” Biochim. Biophys. Acta **1831**(10), 1533–1541 (2013).
3. H. F. Hashemi and J. M. Goodman, “The life cycle of lipid droplets,” Curr. Opin. Cell Biol. **33**, 119–124 (2015).

Optics EXPRESS

4. S. Martin and R. G. Parton, "Lipid droplets: a unified view of a dynamic organelle," Nat. Rev. Mol. Cell Biol. **7**(5), 373–378 (2006).
5. F. Wilfling, J. T. Haas, T. C. Walther, and R. V. Farese, Jr., "Lipid droplet biogenesis," Curr. Opin. Cell Biol. **29**, 39–45 (2014).
6. A. Pol, S. P. Gross, and R. G. Parton, "Biogenesis of the multifunctional lipid droplet: lipids, proteins, and sites," J. Cell Biol. **204**(5), 635–646 (2014).
7. A. S. Greenberg, R. A. Coleman, F. B. Kraemer, J. L. McManaman, M. S. Obin, V. Puri, Q.-W. Yan, H. Miyoshi, and D. G. Mashek, "The role of lipid droplets in metabolic disease in rodents and humans," J. Clin. Invest. **121**(6), 2102–2110 (2011).
8. D. J. Murphy, "The biogenesis and functions of lipid bodies in animals, plants and microorganisms," Prog. Lipid Res. **40**(5), 325–438 (2001).
9. S. J. Wakil and L. A. Abu-Elheiga, "Fatty acid metabolism: target for metabolic syndrome," J. Lipid Res. **50**(Suppl), S138–S143 (2009).
10. H.-K. Kim, M. Della-Fera, J. Lin, and C. A. Baile, "Docosahexaenoic acid inhibits adipocyte differentiation and induces apoptosis in 3T3-L1 preadipocytes," J. Nutr. **136**(12), 2965–2969 (2006).
11. K. Kim, J. Yoon, S. Shin, S. Lee, S.-A. Yang, and Y. Park, "Optical diffraction tomography techniques for the study of cell pathophysiology," J. Biomed. Photonics Eng. **2**(2), 020201 (2016).
12. Y. Sung, W. Choi, C. Fang-Yen, K. Badizadegan, R. R. Dasari, and M. S. Feld, "Optical diffraction tomography for high resolution live cell imaging," Opt. Express **17**(1), 266–277 (2009).
13. J.-W. Su, W.-C. Hsu, C.-Y. Chou, C.-H. Chang, and K.-B. Sung, "Digital holographic microtomography for high-resolution refractive index mapping of live cells," J. Biophotonics **6**(5), 416–424 (2013).
14. S. Shin, K. Kim, T. Kim, J. Yoon, K. Hong, J. Park, and Y. Park, "Optical diffraction tomography using a digital micromirror device for stable measurements of 4-D refractive index tomography of cells," Proc. SPIE **9718**, 971814 (2016).
15. S. E. Lee, K. Kim, J. Yoon, J. H. Heo, H. Park, C. Choi, and Y. Park, "Label-free quantitative imaging of lipid droplets using quantitative phase imaging techniques," in *Asia Communications and Photonics Conference 2014, OSA Technical Digest (online)* (Optical Society of America, 2014), paper ATh1I.3.
16. K. Kim, S. Lee, J. Yoon, J. Heo, C. Choi, and Y. Park, "Three-dimensional label-free imaging and quantification of lipid droplets in live hepatocytes," Sci. Rep. **6**(1), 36815 (2016).
17. K. Czamara, K. Majzner, M. Z. Pacia, K. Kochan, A. Kaczor, and M. Baranska, "Raman spectroscopy of lipids: a review," J. Raman Spectrosc. **46**(1), 4–20 (2015).
18. H. Wu, J. V. Volponi, A. E. Oliver, A. N. Parikh, B. A. Simmons, and S. Singh, "In vivo lipidomics using single-cell Raman spectroscopy," Proc. Natl. Acad. Sci. U.S.A. **108**(9), 3809–3814 (2011).
19. X. Nan, J.-X. Cheng, and X. S. Xie, "Vibrational imaging of lipid droplets in live fibroblast cells with coherent anti-Stokes Raman scattering microscopy," J. Lipid Res. **44**(11), 2202–2208 (2003).
20. C. Cao, D. Zhou, T. Chen, A. M. Streets, and Y. Huang, "Label-free digital quantification of lipid droplets in single cells by stimulated Raman microscopy on a microfluidic platform," Anal. Chem. **88**(9), 4931–4939 (2016).
21. W.-C. Hsu, J.-W. Su, T.-Y. Tseng, and K.-B. Sung, "Tomographic diffractive microscopy of living cells based on a common-path configuration," Opt. Lett. **39**(7), 2210–2213 (2014).
22. Y. Kim, H. Shim, K. Kim, H. Park, J. H. Heo, J. Yoon, C. Choi, S. Jang, and Y. Park, "Common-path diffraction optical tomography for investigation of three-dimensional structures and dynamics of biological cells," Opt. Express **22**(9), 10398–10407 (2014).
23. T. Ikeda, G. Popescu, R. R. Dasari, and M. S. Feld, "Hilbert phase microscopy for investigating fast dynamics in transparent systems," Opt. Lett. **30**(10), 1165–1167 (2005).
24. A. Rohwedder, Q. Zhang, S. A. Rudge, and M. J. Wakelam, "Lipid droplet formation in response to oleic acid in Huh-7 cells is mediated by the fatty acid receptor FFAR4," J. Cell Sci. **127**, 3104–3115 (2014).
25. A. Herms, M. Bosch, N. Ariotti, B. J. N. Reddy, A. Fajardo, A. Fernández-Vidal, A. Alvarez-Guaita, M. A. Fernández-Rojo, C. Rentero, F. Tebar, C. Enrich, M.-I. Geli, R. G. Parton, S. P. Gross, and A. Pol, "Cell-to-cell heterogeneity in lipid droplets suggests a mechanism to reduce lipotoxicity," Curr. Biol. **23**(15), 1489–1496 (2013).
26. L. L. Listenberger, X. Han, S. E. Lewis, S. Cases, R. V. Farese, Jr., D. S. Ory, and J. E. Schaffer, "Triglyceride accumulation protects against fatty acid-induced lipotoxicity," Proc. Natl. Acad. Sci. U.S.A. **100**(6), 3077–3082 (2003).
27. I. W. Schie, L. Nolte, T. L. Pedersen, Z. Smith, J. Wu, I. Yahiatène, J. W. Newman, and T. Huser, "Direct comparison of fatty acid ratios in single cellular lipid droplets as determined by comparative Raman spectroscopy and gas chromatography," Analyst (Lond.) **138**(21), 6662–6670 (2013).
28. T. Plötz, M. Hartmann, S. Lenzen, and M. Elsner, "The role of lipid droplet formation in the protection of unsaturated fatty acids against palmitic acid induced lipotoxicity to rat insulin-producing cells," Nutr. Metab. (Lond.) **13**(1), 16 (2016).
29. A. S. Rambold, S. Cohen, and J. Lippincott-Schwartz, "Fatty acid trafficking in starved cells: regulation by lipid droplet lipolysis, autophagy, and mitochondrial fusion dynamics," Dev. Cell **32**(6), 678–692 (2015).